



# Assessing Water and Sand Inrushes Hazard Reductions due to Backfill Mining by Combining GIS and Entropy Methods

Yong Liu<sup>1</sup> · Jiawei Liu<sup>2</sup> · Binbin Yang<sup>3</sup> · Shichong Yuan<sup>1</sup>

Received: 8 September 2020 / Accepted: 11 September 2021 / Published online: 22 September 2021  
© Springer-Verlag GmbH Germany, part of Springer Nature 2021

## Abstract

Backfill coal mining, an environmentally friendly practice, is widely used to mitigate the hazards of water and sand inrushes (WSIs) and surface subsidence. In this study, a quantitative analysis for assessing the hazard reduction of WSIs due to backfilling was established that combines a modified analytic hierarchy process (AHP) with a geographic information system (GIS) and entropy. The analytical and quantitative model consists of four criteria and eight factors for the hazard assessment target layer. The weight of each index is comprehensively determined based on the modified AHP and entropy. Then, a hazard zone map that is color-coded is overlay analyzed based on GIS to comparatively evaluate the degrees of hazard from WSI due to longwall caving and paste backfill. The Taiping coal mine was used as a case study to validate the accuracy of the evaluation model. The results indicate that paste backfilling can effectively reduce the influence of the overburden failure height on WSI hazards. The highest hazard index of backfill mining was significantly reduced, and high-hazard and very high-hazard zones of longwall caving were transformed into low-hazard or even no-hazard zones. The evaluation results are in good agreement with actual engineering practices and offer an effective reference for practical engineering projects and prevention and control measures for safe mining under loose sand aquifers.

**Keywords** Backfill mining under aquifers · Water and sand inrushes (WSIs) · Analytic hierarchy process · Weight · Hazard degree

## Introduction

Coal mining under water bodies has been seriously threatened by water and sand inrush (WSI) disasters due to the removal of materials that creates large voids underground (Fan et al. 2019; Hou et al. 2019). The resulting voids also induce surface subsidence and damage the integrity and continuity of the overlying rock and soil layers, which can cause great economic losses and many human casualties (Li et al. 2019a; Zhu et al. 2016). To ensure the safety of coal mining underground, backfilling has become an effective method to mitigate and address these geological disasters and societal issues (Deng et al. 2017; Huang et al. 2018).

In recent years, surveys on strata movement and deformation and control of surface subsidence due to backfill mining have been theoretically and experimentally studied (Zhang et al. 2015; Zhu et al. 2019). Moreover, the deformation and stress state of backfill materials and the factors that influence them have already been investigated by multiphysics modeling and simulation and experimental methods (Doherty et al. 2015; Li et al. 2019b). Previous research has indicated

✉ Jiawei Liu  
20201007@hncj.edu.cn

✉ Binbin Yang  
yangbinbin@xcu.edu.cn

Yong Liu  
cumtliu@126.com

Shichong Yuan  
yuan920620@hotmail.com

<sup>1</sup> Institute of Mine Water Hazards Prevention and Controlling Technology, School of Resources and Geosciences, China University of Mining and Technology, 1 University Rd, Xuzhou 221116, Jiangsu, China

<sup>2</sup> School of Civil and Transportation Engineering, Henan University of Urban Construction, Longxiang Road, Xincheng Area, Pingdingshan 467036, Henan, China

<sup>3</sup> School of Civil Engineering, Xuchang University, 88 Bayi Rd, Xuchang 461000, Henan, China

that backfill mining can mitigate the development of the height of overburden failure, which is an important parameter in predicting and preventing WSI disasters, preserve water resources, and protect the ecological environment (Liu et al. 2017; Sui et al. 2015; Sun et al. 2018).

However, in complex hydrogeological and geological conditions, the hazards of WSIs associated with mining under loose layers of sediment is substantially increased, and predicting and assessing the degree to which the hazard is reduced by backfill mining can be challenging (Polak et al. 2016; Babos et al. 2019; Xu et al. 2019). The primary factor for assessing the hazard degree is the height of the water-conducting fractured zone, which can be predicted using numerical simulation, drilling, field investigation including water injection and three-dimensional seismic experiments, and transient electromagnetic analysis based on a constitutive model (Li et al. 2019c; Zhang et al. 2014, 2018). Furthermore, nonlinear methods such as the vulnerability index evaluation system combined with AHP and ANN were comprehensively established in the GIS environment and successfully applied for risk assessment of water inrush (Wu et al. 2008, 2011). Yang et al. (2017) constructed a fuzzy comprehensive evaluation model combining GIS and entropy weight to evaluate the risk of water inrush due to coal mining above aquifers.

Moreover, conventional methods for determining the likelihood of inrushes fail to consider the complexities of the factors that affect sand collapse while backfilling, which makes predicting the occurrence of inrushes accurately and quantitatively challenging. Several key factors, such as the thickness of the overburden, geological structure, water abundance of the aquifers, and height of overburden failure, need to be overlain and analyzed to investigate their interactions and evaluate their influence on the inrush hazard due to the different correlations between the different factors. Therefore, we decided to determine and quantitatively evaluate the spatial distribution characteristics of these key factors to evaluate their degree of influence on inrush hazards. An evaluation index was first constructed by identifying the main controlling factors that affect WSIs. Then, single factor modeling analysis was conducted for each controlling factor. A quantitative method of analysis for the inrush hazard due to backfill mining under loose sand layers was established, which was used to comparatively analyze the results of backfill mining and longwall caving. Finally, a quantitative method for analyzing and assessing the hazard of inrushes due to backfill mining under an aquifer with loose sand was established, which can be used as a preventive and control measure for mining safely under an aquifer with loose sand.

## Materials and Methodology

### Geological Conditions

A quantitative analysis was carried out on paste backfill under a loose layer of sediment in the 6th mining district in the southern region of the Taiping coal mine, Jinling city, Jiangsu Province, China (Fig. 1). The no. 3 coal seam is primarily exploited in this mine; it has an average thickness of 8.4 m and a simple geological structure. The layout of the panels of the Taiping coal mine is shown in Fig. 2. Four panels were examined in the study area (panels S01, S02, S03, and S04) and three mined slices were paste backfilled in each panel. Caving was carried out in the first slice with a mined thickness of 1.8 m, while the other two slices were mined at thicknesses of 2.2 m. In total, 114 boreholes were drilled in the study area, which provided data on the geological and hydrogeological conditions. The results of the field work indicated that the thickness of the clay layer at the bottom of the Quaternary deposits ranges from 0.7 to 14.02 m, with an average of 3.6 m, which serves to protect the aquifer during mining. The thickness of the overburden ranged between 5.3 and 32.6 m, with an average of 22.3 m. The water abundance of the aquifer has a specific capacity that ranged between 0.03 and 0.11 L/(s m) with an average of 0.08 L/(s m), which is low to intermediate (State Administration of Coal Mine Safety 2018). The hydraulic conductivity ranged from 0.17 to 0.34 m/day, with an average of 0.25 m/day.

### Methodology

A schematic of the quantitative method of analysis that combines both the entropy method and the modified AHP is shown in Fig. 3. An evaluation index is first established, followed by individual evaluation of each factor index using GIS to produce thematic maps. The normalization process is shown according to Eq. (1).

$$\begin{cases} x' = -x_i \\ y = \frac{(x - \text{MinValue})}{(\text{MaxValue} - \text{MinValue})} \end{cases} \quad (1)$$

where  $x'$  indicates a positive quantized value;  $x_i$  is the original negative correlation index value;  $x$  and  $y$  are the index values before and after processing, respectively; and  $M_{ax}Value$  and  $M_{in}Value$  are the maximum and minimum index values of the samples, respectively.

Weight is a sensitivity parameter that is used to verify the importance of each index (Li et al. 2013). The weight of each factor index was determined by the entropy method and a modified AHP. AHP weighting is a pairwise



**Fig. 1** Location of Taiping coal mine

comparison method for decision making that was first proposed by Saaty (1980) and disaggregates decisions into different hierarchical levels. The judgment matrix can be obtained according to the expertise score (Eq. 2).

$$A = [a_{ij}]_{n \times n} \quad (2)$$

where  $A$  is a positive and reciprocal matrix and the normalized eigenvector of  $A$  can be used as a weight vector. Otherwise, the eigenvector of the largest eigenvalue  $\lambda$  of matrix  $A$  can be used as the weight vector (Eq. 3).

$$Aw = \lambda_{\max} w \quad (3)$$

where  $\lambda_{\max}$  is the largest eigenvalue of matrix  $A$ . The weights can be calculated based on Eqs. (4) and (5).

$$w_i = \frac{\sum_{j=1}^n C'_{ij}}{n}, \quad i = 1, 2, \dots, n \quad (4)$$

$$W = \begin{bmatrix} w_1 \\ w_2 \\ \vdots \\ w_n \end{bmatrix} = \begin{bmatrix} \frac{1}{n} \sum_{k=1}^n C'_{1n} \\ \frac{1}{n} \sum_{k=2}^n C'_{2n} \\ \vdots \\ \frac{1}{n} \sum_{k=n}^n C'_{nn} \end{bmatrix} \quad (5)$$

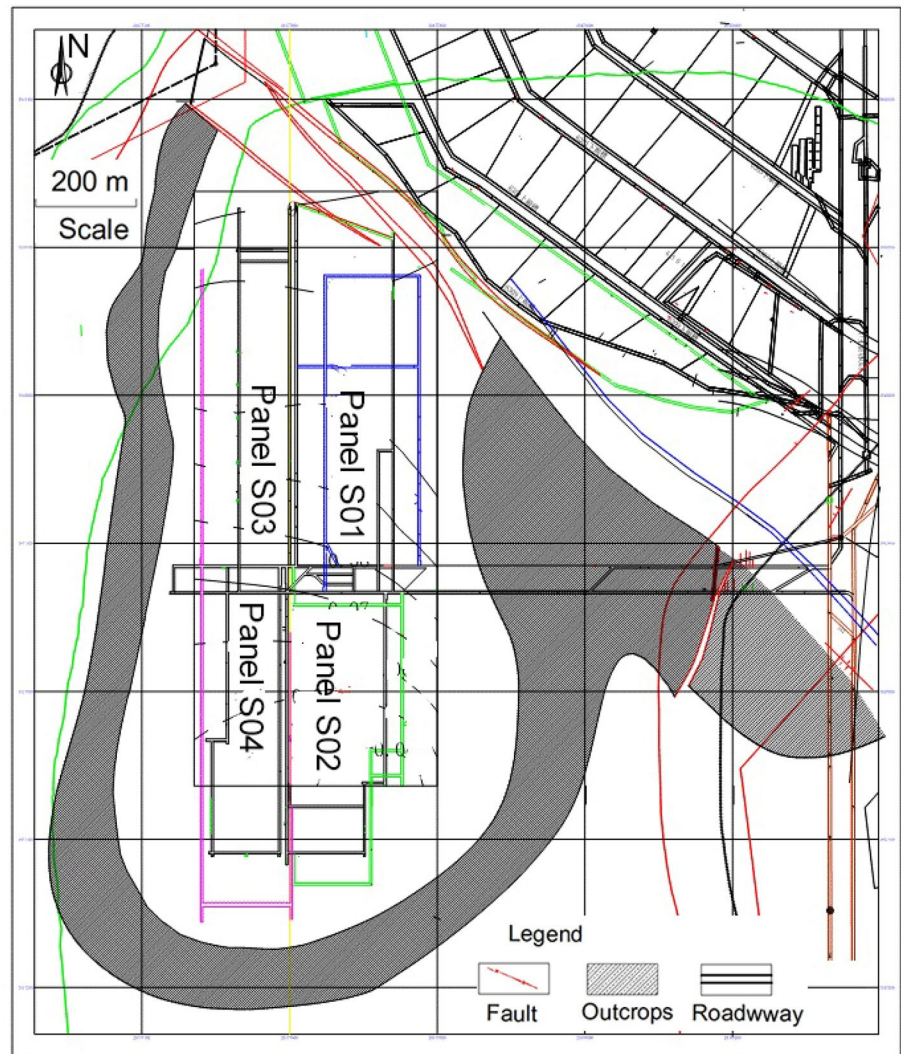
$$C'_{ij} = \frac{C_{ij}}{\sum_{i=1}^n C_{ij}}, \quad i = 1, 2, \dots, n \quad (6)$$

Entropy weight (EW) has been widely adopted for quantitatively determining the effects of sample statistics, and reveal the relationships of EW with the sample mean, standard deviation (SD), and coefficient of variation (CV) (Wu et al. 2015). The entropy method is an accurate and objective mathematical model to calculate the weights of factors, and the calculation mathematical model (Eq. 7).

$$\begin{cases} P_{ij} = \frac{x_{ij}}{\sum_{i=1}^n x_{ij}}, \quad (i = 1, 2, \dots, n; j = 1, 2, \dots, m) \\ e_j = -k \sum_{i=1}^n p_{ij} \ln(p_{ij}), \quad k > 0, \quad k = \frac{1}{\ln(m)}, \quad e \geq 0 \\ g_j = \frac{1-e_j}{m-E_e}, \quad E_e = \sum_{j=1}^m e_j, \quad 0 \leq g_j \leq 1, \quad \sum_{j=1}^m g_j = 1 \\ w_j = \frac{g_j}{\sum_{j=1}^m g_j} \quad (1 \leq j \leq m) \end{cases} \quad (7)$$

where  $x_{ij}$  is the value of the  $i$ th evaluation object on the  $j$ th evaluation index,  $p_{ij}$  is the proportion of the  $i$ th evaluation object index value under the  $j$ th index,  $e_j$  is the entropy weight of the  $j$ th index,  $E_e$  is the summed entropy weights of each index,  $g_j$  is the difference coefficient of the  $j$ th index (the larger the  $g_j$  value is, the greater the entropy weight of

**Fig. 2** Layout of panels in the 6th mining district to south of Taiping Coal Mine



the index) and  $w_j$  is the entropy weight coefficient of the  $j$ th index.

Combining this approach with the entropy method proposed by Yang et al. (2019) would be more appropriate for determining the weight of each criterion. The evaluation index weight is determined by the weighted average according to the calculated results of the two methods. According to the established evaluation matrix, the weight calculated based on the AHP method is recorded as weight 1, and the weight calculated based on the information entropy method is recorded as weight 2. Averaging weights 1 and 2 yields the final evaluation factor.

Finally, a hazard zone map is produced after an overlay analysis was performed with GIS to quantify the degree of hazard associated with paste backfill mining under an aquifer with loose sand in the Taiping Coal Mine. The backfill mining hazard index (BMHI) quantifies the hazard degree of WSI due to paste backfill under an aquifer with loose sand, as shown in Eq. (8):

$$BMHI = \sum_{v=1}^n w_v (f_{uv}) \quad (8)$$

where  $w_v$  is the weight of the criterion and  $f_{uv}$  is the value function. The evaluation results are classified using the natural breaks method based on the definition of the BMHI and are shown as  $G = (0.3, 0.45, 0.65, 0.80, \text{ and } 0.95)$ , which denote no hazard, low hazard, moderate hazard, high hazard, and very high hazard zones, respectively.

### Identifying the Criteria for Each Factor

Coal mining under an aquifer with loose sand can incur WSI hazards, as exemplified in many mining-induced tragedies. Many different factors contribute to the inrush hazard with different degrees of influence, including the: unevenness of the bedrock surface, fractal dimension of faults, thickness of the overburden and clay layer at the bottom of the



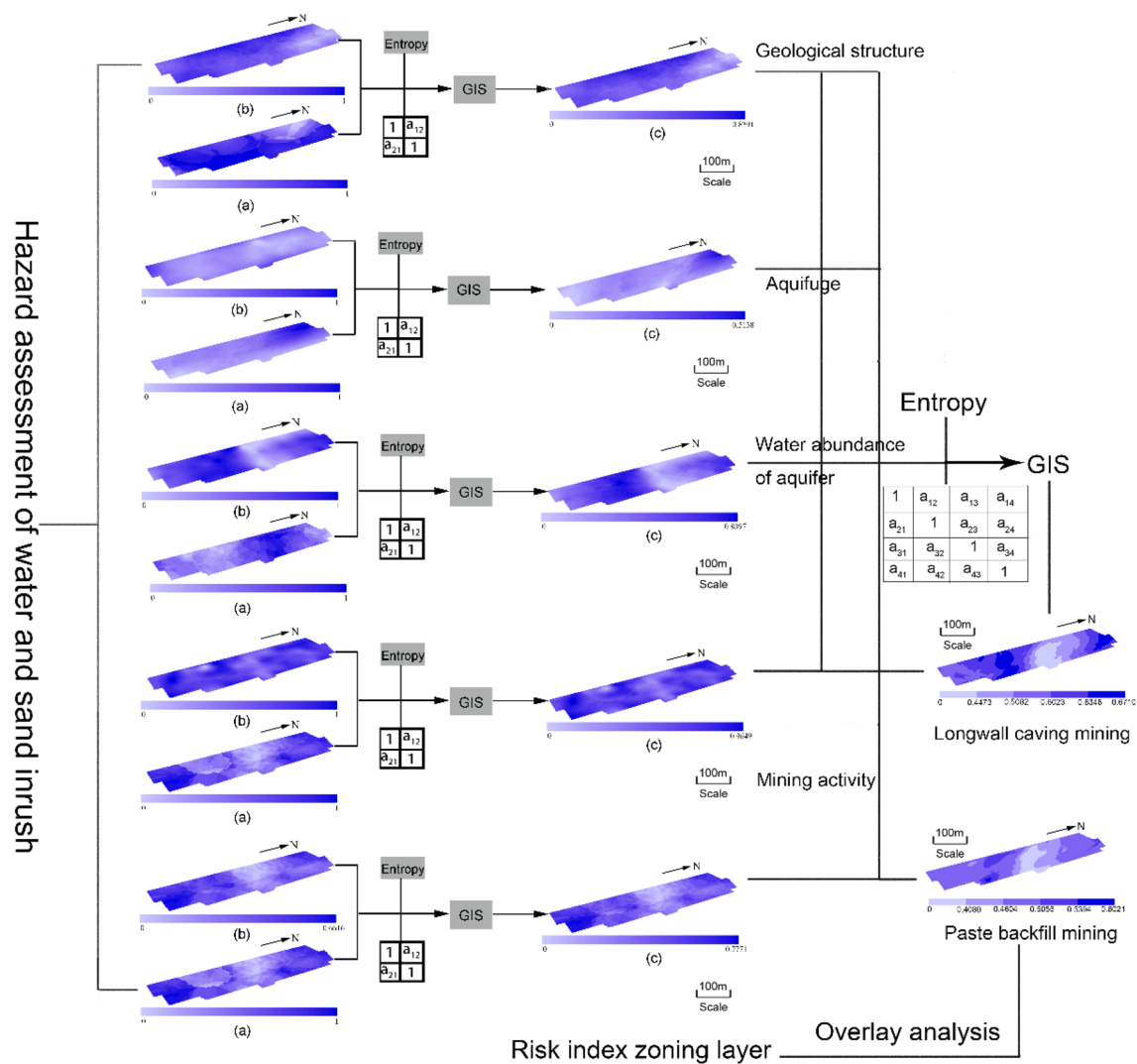


Fig. 3 Flowchart of AHP method

Quaternary deposits, specific capacity and hydraulic conductivity of the aquifer, mined thickness, and height of the overburden failure. The four criterion layers for evaluation include the geological structure, aquifuge, water abundance of the aquifer, and mining activity. A schematic for quantitatively evaluating the WSI hazard is shown in Fig. 3.

The unevenness of the bedrock surface is significantly affected by faults that can act as channels for the infiltration of water and sand. The overburden is susceptible to mining activities due to the unevenness of the bedrock surface; the integrity and continuity of the overburden are reduced and the integrity of the aquifuge is decreased, which increases the inrush hazard occurrence. A thick aquifuge between a mined coal seam and an aquifer with loose sand may effectively prevent the water-conducting fractured zone from penetrating the aquifer, while the

fracturing of a thinner aquifuge may provide channels for water and sand flow. The specific capacity is the main index for showing the storage capacity of an aquifer and the hydraulic conductivity is an important indicator of the permeability of the rock and soil. The hydraulic conductivity is also an important parameter of an aquifer, as it indicates the permeability of the rock and soil. Low water abundance may indicate low hydraulic conductivity of an aquifer, and a high water level indicates high hydraulic conductivity. The height of overburden failure is significantly and directly related to the mining thickness. That is, when the mining thickness is increased, more severe overburden failure occurs, which allows the water-conducting fractured zone to reach the overlying aquifer. These factors all increase the inrush hazard.

## Results and Discussion

### Quantification of the Evaluation Factor

#### Fluctuation of the Bedrock Surface and Fractal Dimensions of Faults

A more uneven bedrock surface can contribute to a greater inrush hazard when mining under an aquifer with loose sand, which means that the unevenness of the bedrock structure and inrushes are positively correlated and can be directly normalized. A thematic map of the unevenness of the bedrock surface was produced (Fig. 4a). The bedrock surface is more uneven due to weathering in the center of the western region and in the southeastern region than in other parts of the study area; these places are also near the coal seam outcrops, thus indicating a higher inrush hazard. Generally, the bedrock surface is slightly uneven in most of the study area, especially where Panel S01 is located, which indicates that the bedrock surface has little influence on the risk of inrush occurrence.

The fractal dimension, which is a ratio that compares pattern changes, is used as a measure of the complexities of changes in faults based on fractal theory. The similarity dimension ( $D_s$ ) is used to quantify the influence of faults on inrush hazards and is calculated using mesh coverage as shown in Eq. (9):

$$D_s = -\lg N(d) / \lg d \quad (9)$$

where  $d$  is the diameter of the point set and  $N(d)$  is the minimum number of units that can be covered by the mesh.

A larger fractal dimension indicates a higher inrush hazard. The thematic map is shown in Fig. 4b. The areas with larger fractal dimensions are mainly found on the eastern side of the study area, where Panels S01 and S02 are located. A number of small faults are exposed in the open cut wall of Panel S01, which naturally separate the northern and southern areas in the Taiping coal mine. Moreover, several faults were found in the road to Panel S02 during the excavation process, especially in the lower road, which is close to the coal seam outcrops; therefore, the road was redesigned to avoid these faults. However, most of the throws are less than 5 m, and the faults are mainly spatially distributed in the excavation road; these factors indicate that the fault structure is simple, and the scale of the faults is small.

#### Thickness of the Overburden and Clay Layer at the Bottom of the Quaternary Deposits

The thickness of the overburden is negatively correlated with the effect of mining a coal seam under a thin layer of bedrock

and a thick aquifer with loose sand; a thick overburden can effectively reduce the WSI hazard. Based on its distribution in the study area, the overburden thickness is thematically mapped in Fig. 4c. The obtained borehole information indicates that the overburden in most parts of the study area is less than 40 m thick, which means that it is a thin layer. The overburden is uniformly distributed in the study area, except for the corner of the southwestern region and the eastern part of the mine, which have very thin overburdens due to weathering and crosscutting faults, respectively.

The thickness of the clay layer at the bottom of the Quaternary deposits is also negatively correlated with the effect of mining under a thin layer of bedrock and a thick aquifer with loose sand, and a thick clay layer can effectively reduce the inrush hazard. The thematic map of the clay layer distribution is shown in Fig. 4d. The clay layer is spatially widespread throughout the study area, and mining does not affect its integrity, which greatly inhibits inrush. Only in the northwestern region of the study area, where the spatial distribution of the clay layer is the lowest (zero) in Panel S03, is there a greater risk; this is consistent with the geological conditions.

#### Specific Capacity and Hydraulic Conductivity of the Aquifer

The loose sand aquifer in the lower layers of the Quaternary deposits is composed of coarse gravel and sand. Moreover, the clay and sand layers are interstratified. The borehole information shows that the specific capacity of the aquifer ranges between 0.02 L/(s m) and 0.20 L/(s m) and is unevenly distributed. Furthermore, the water head ranges from 64.3 to 74.3 m on top of the bedrock surface and averages 69.3 m. Thus, the water abundance of the loose sand aquifer is low to moderate (State Administration of Coal Mine Safety 2018).

The specific capacity of the aquifer shows a positive correlation with the effect of mining under a thin layer of bedrock, and a thick aquifer with loose sand increases the inrush hazard. The specific capacity of the aquifer was thematically mapped based on the drilling and pumping test results in the study area (Fig. 4e). A larger specific capacity could be due to surface water recharge in the northwestern region of the study area, which is near the coal seam outcrops and a thinner clay layer. Furthermore, strata with numerous porous structures may provide channels for water and sand flow due to crosscutting by small faults in the center of the study area. A number of drainage holes may also contribute to a larger specific capacity in the center of the study area. In general, the study area has low to moderate levels of water abundance and low hydraulic connectivity between the aquifers.

The hydraulic conductivity of the aquifer is positively correlated with the effect of mining under a thin layer of bedrock, and again, the presence of a thick aquifer with

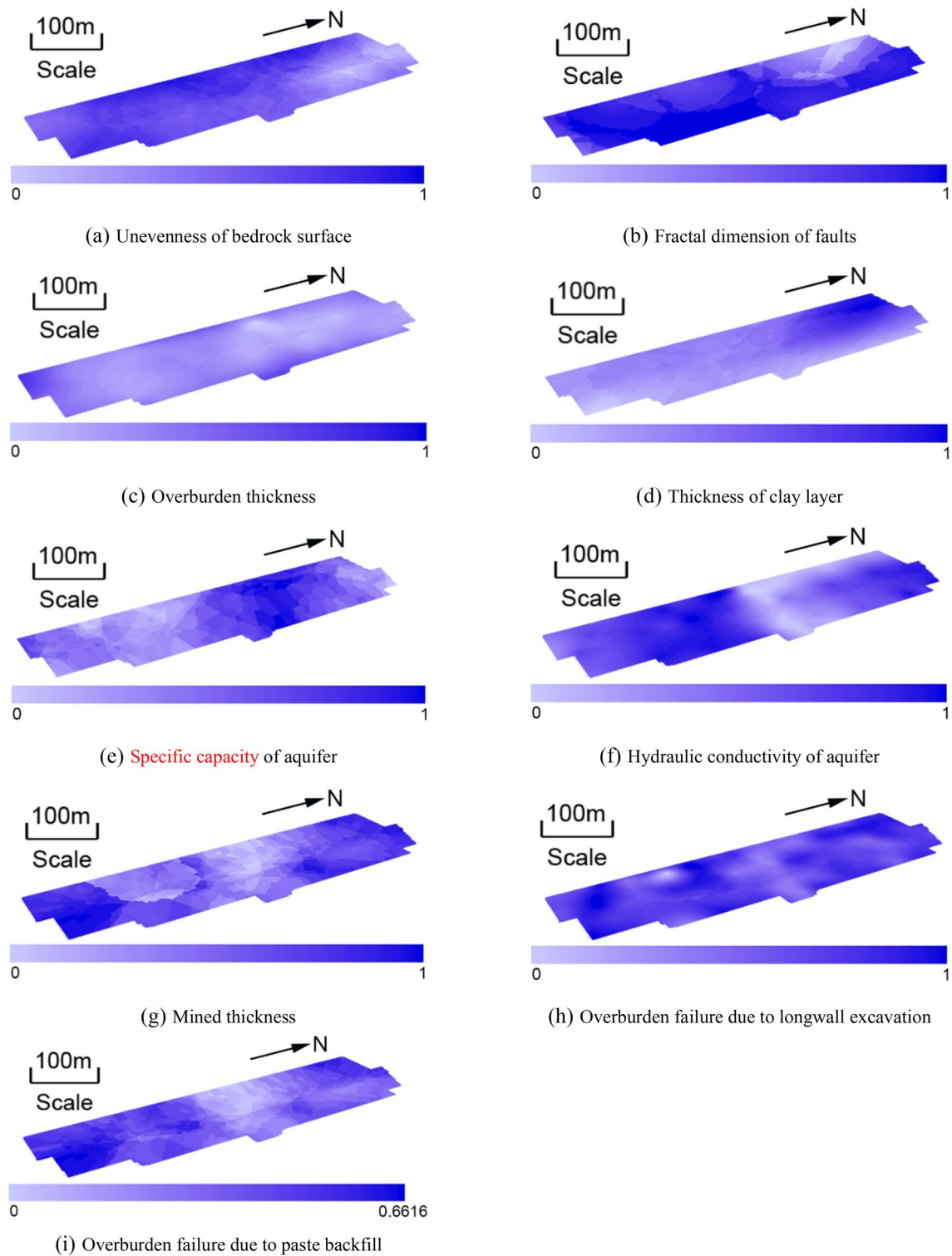


**Fig. 4** Thematicmap of each evaluation factor. **a** Unevenness of bedrock surface; **b** fractaldimension of faults; **c** overburden thickness; **d** thickness of clay layer; **e** specific capacity of aquifer; **f** hydraulic-

conductivity of aquifer; **g** mined thickness; **h** overburden failure due tolongwall excavation; **i** overburden failure due to paste backfill

loose sand increases the inrush hazard. The hydraulic conductivity is thematically mapped in Fig. 4f based on the drilling and pumping test results in the study area. The center of the study area shows a lower hydraulic conductivity, which indicates less risk. In terms of the geological conditions, the axial part of a syncline with a northeastward plunge has relatively low permeability. In addition, small faults have developed south of the study area, which increases hydraulic conductivity. Objectively, the aquifer has low permeability and is non-uniform, which may increase the inrush hazard.

### Mined Thickness and Height of Overburden Failure

Mining is also a main controlling factor for the occurrence of WSIs in coal mines. Once mining commences, the water-conducting fractured zone, including the caved and fractured zones, may provide channels for the migration of water and sand and finally cause an inrush due to overburden failure. Thus, changes to the goaf properties due to mining are the fundamental reason for overburden failure.

The study area has typical mining conditions for this area, in which a thick coal seam is mined under a thin layer of bedrock. It is important that the multiple slices are backfilled to prevent overburden failure and decrease ground subsidence to reduce or eliminate any negative effects on the ecological environment at the ground surface for environmentally favorable and sustainable development. Practically, the mined thickness was positively correlated with the inrush hazard, which means that when the mined thickness increases, the inrush hazard is greater. The mined thickness is thematically mapped based on field work carried out in the study area (Fig. 4g). The mined thickness is greater in the northern and southern regions due to the unevenness of the coal seam floor, which significantly increases the WSI hazard. In addition, differences in the construction process can also cause an increase in the mined thickness in the center of the study area.

The height of overburden failure is positively correlated with the effect of mining under a thin layer of bedrock, and the thick aquifer with loose sand increases the inrush hazard. The height of overburden failure due to longwall excavation is thematically mapped based on field work in the study area (Fig. 4h). This factor index is high and distributed very unevenly in the study area, which seriously threatens the safety of mining and increases the risk of inrushes.

The height of overburden failure was calculated based on Eq. (10) (State Administration of Security Supervision et al. 2017). The optimal backfill thickness ranges from 1.75 to 2 m with an average thickness of 1.86 m for an actual mined thickness of 2.2 m based on field work results in Liu et al. (2017).

$$\begin{cases} H_f = \frac{100 \sum M}{1.6 \sum M+3.6} \pm 5.6, & (\text{for moderate to hard and hard rock}) \\ H_f = \frac{100 \sum M}{3.1 \sum M+5.0} \pm 4.0, & (\text{for soft rock}) \end{cases} \quad (10)$$

The overburden failure of paste backfill was thematically mapped using the GIS spatial analysis function (Fig. 4i). The weathering and unevenness of the overburden contributes to the poor overburden integrity, which is likely to cause movement of the rock layer. Moreover, the small faults in the southern region of the mine increase the amount of overburden failure. However, paste backfilling can effectively reduce the height of overburden failure compared to longwall caving. In general, the effect of overburden failure on the WSI hazard was significantly reduced by paste backfilling in most of the study area.

### Establishment of the Evaluation Matrix

According to the hierarchical structure of the hazard factors for WSI that were determined based on the geological conditions, the weight of each factor was calculated based on the AHP and entropy method. A matrix for the evaluation of the criterion layers and factor indexes was constructed and shown below. Equation (11) shows the matrix for the evaluation of the criterion layers:

$$\begin{bmatrix} 1.000 & 0.125 & 0.167 & 3.000 \\ 8.000 & 1.000 & 2.000 & 0.250 \\ 5.999 & 0.5000 & 1.000 & 0.500 \\ 0.333 & 4.000 & 2.000 & 1.000 \end{bmatrix} \quad (11)$$

where the matrix of the aquifuge and the water abundance of the aquifer are shown by Eqs. (12) and (13), respectively.

$$\begin{bmatrix} 1.000 & 2.500 \\ 0.400 & 1.000 \end{bmatrix} \quad (12)$$

$$\begin{bmatrix} 1.000 & 1.600 \\ 0.625 & 1.000 \end{bmatrix} \quad (13)$$

Specifically, the criterion layer of mining activity mainly includes the mined thickness and the height of overburden failure. To determine the difference between longwall caving and paste backfilling, two matrices were built for the evaluation, as shown in Eqs. (14) and (15), respectively.

$$\begin{bmatrix} 1.000 & 1.200 \\ 0.833 & 1.000 \end{bmatrix} \quad (14)$$

$$\begin{bmatrix} 1.000 & 0.650 \\ 1.538 & 1.000 \end{bmatrix} \quad (15)$$



## Weight of the Evaluation Index

The weight of the evaluation index is determined by using the calculated results from the AHP and entropy methods, which are labeled weights 1 and 2, respectively. Then, the final weight of each factor is obtained by weighting and averaging the results. The calculated weights of the four criteria are provided in Table 1. Among these four criteria, the geological structure has the lowest weight of 0.1092, which indicates a small influence on the inrush hazard because the study area has a relatively simple geological structure. The aquifuge has the highest weight of 0.3321, followed by mining activity with a weight of 0.2984 and water abundance with a weight of 0.2603. The hazard is reduced if the aquifuge is thicker than the height of overburden failure, since there are no channels for water and sand flow even with high water levels and during mining of a thick layer of coal. Thus, the thickness of the aquifuge has the most influence on the inrush hazard in the study area.

The weights of the factors are listed in Table 2. In terms of the geological structure, the unevenness of the bedrock surface has a higher weight due to weathering in the area near the coal seam outcrops since there is a simple, small-scale fault structure in the study area. The weight of  $\approx 0.64$  for the clay layer of the aquifuge in the Quaternary deposits is important since it is higher than the overburden thickness index and therefore inhibits the inrush hazard. The specific capacity and hydraulic conductivity have weights of 0.54 and 0.46, respectively, i.e. the specific capacity is slightly more important than the hydraulic conductivity. Since paste

backfill can effectively reduce the height of overburden failure and mitigate the bedrock subsidence hazard, the weight of the overburden failure height is reduced from 0.59 to 0.53 with the entropy method.

## Final Evaluation and Comparative Analysis of Inrush Hazard due to Longwall Caving and Paste Backfill

Figure 5 shows the thematic map of the geological structure. Most of the study area is in a zone where there is no to moderate inrush hazard. The only high inrush hazard zone is small and found in the western part of the study area, close to where the seam outcrops, and where the highly elevated bedrock was seriously affected by weathering and erosion, which increases the WSI hazard.

Figure 6 shows the thematic map of the aquifuge contribution to the WSI hazard. Most of the study area has no inrush hazard. The maximum hazard index is only 0.5138, which is found in the northeastern corner of the study area, in a zone with a low inrush hazard. Specifically, the low-hazard zone is found in the boundaries between the southern and northern districts of the 6th mining district, where there is a certain degree of disturbance due to the adjacent mining.

The highest weight of the water abundance of the aquifer on the inrush hazard is 0.8097. The region with a high inrush hazard is found in the center of the study area, and most of the other parts are zones with no or low inrush hazard, as shown in Fig. 7. Due to multiple slice mining for long periods of time, the geological structure south of the study area has loose sediment, which increases the specific capacity

**Table 1** Weight of each criterion

Criterion	Weight 1	$\lambda_{max}$	CI	Entropy	Weight 2	Weight
Geological structure	0.1163	6.8703	0.9568	0.9922	0.1021	0.1092
Aquifuge	0.3290			0.9744	0.3352	0.3321
Water abundance	0.2574			0.9799	0.2632	0.2603
Mining activity	0.2973			0.9771	0.2996	0.2984

**Table 2** Weight of factors in each criterion layer

Criterion layer	Factor	Weight 1	$\lambda_{max}$	CI	Entropy	Weight 2	Weight
Geological structure	Unevenness of bedrock surface	0.7143	2	0	0.9713	0.784153	0.749219
	Fractal dimension of faults	0.2857			0.9921	0.215847	0.250781
Aquifuge	Thickness of clay layer	0.6154	2	0	0.9814	0.657244	0.636314
	Thickness of overburden	0.3846			0.9903	0.342756	0.363686
Water abundance of aquifer	Specific capacity	0.5455	2	0	0.9771	0.535047	0.540251
	Hydraulic conductivity	0.4545			0.9801	0.464953	0.459749
Mining activity (longwall caving)	Mined thickness	0.3939	2	0	0.9854	0.41954	0.40674
	Height of overburden failure	0.6061			0.9798	0.58046	0.59326
Mining activity (paste backfilling)	Mined thickness	0.3939	2	0	0.9798	0.5445	0.4692
	Height of overburden failure	0.6061			0.9831	0.4555	0.5308

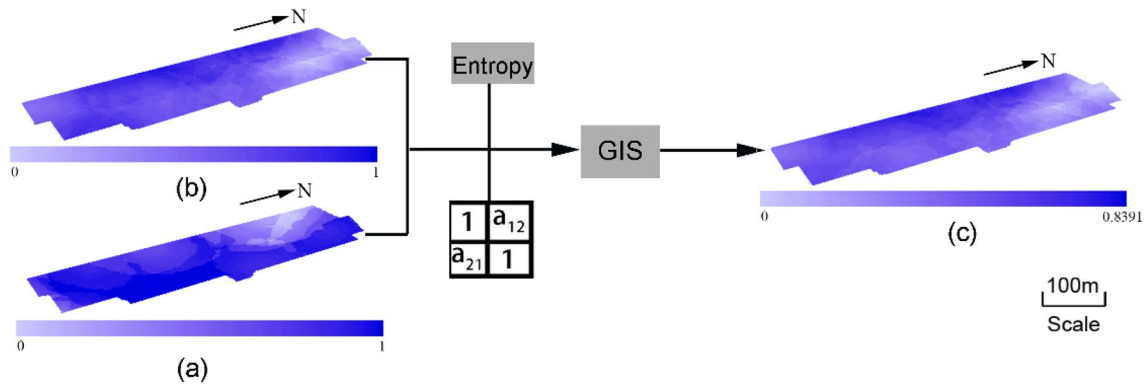


**Fig. 5** Thematicmap of criterion layer—geological structure. **a** Unevenness of bedrock surface; **b** fractal dimension of faults

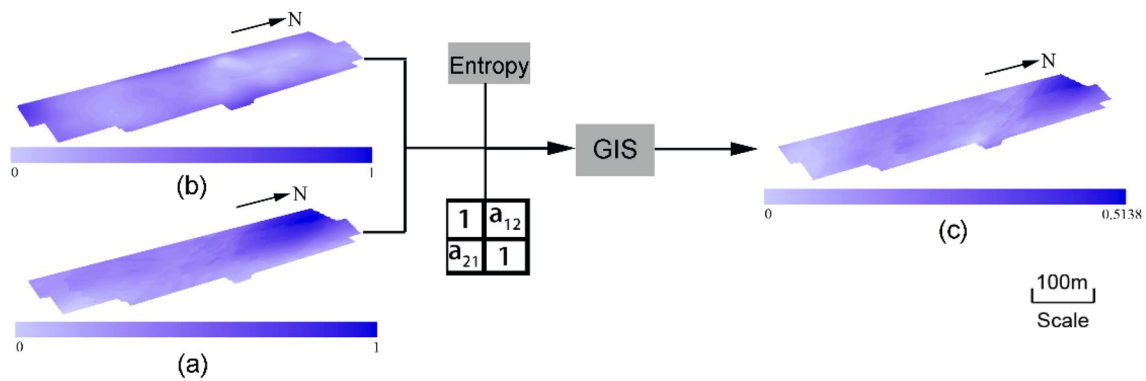


**Fig. 6** Thematic map of criterion layer—aquifuge. **a** Overburden thickness; **b** thickness of clay layer at bottom of quaternary deposit

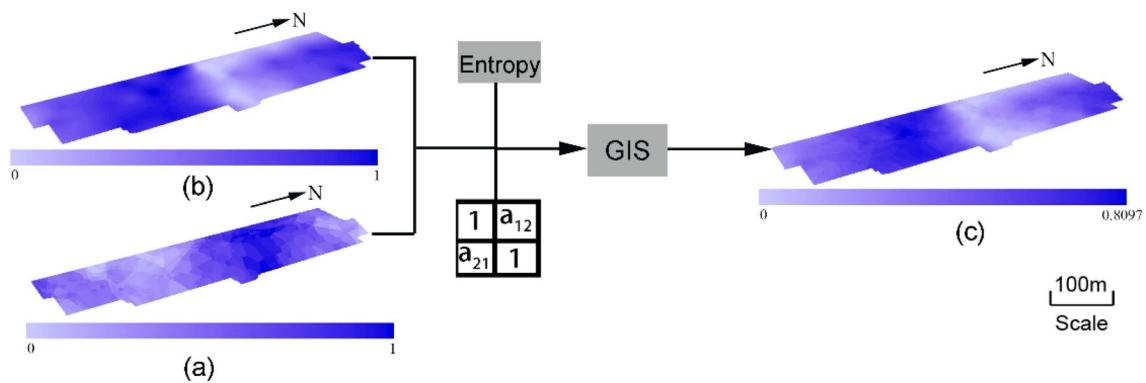


**Fig. 7** Thematicmap of criterion layer—water abundance of aquifer. **a** Specific capacity; **b** hydraulic conductivity

and hydraulic conductivity of the aquifer and increases the WSI hazard. The inrush hazard in the southern part of the study area is generally greater than in the northern part.

The hazard index of WSI due to longwall caving is up to 0.9649 with the overlay analysis and most of the study area lies within high-hazard zones, which means that the mining method greatly increases the inrush hazard (Fig. 8). After paste backfilling, the hazard index was

reduced to 0.7771, and most of the other areas were low-hazard zones, except for the southeastern and northwestern corners of the study area, which are moderate-hazard zones. As a result, paste backfilling effectively reduces the hazard index of inrushes, as shown in Fig. 9. Panel S02 in the 6th mining district was the first to carry out paste backfilling. After longwall caving of the first slice, which significantly affected the overburden, paste backfilling was

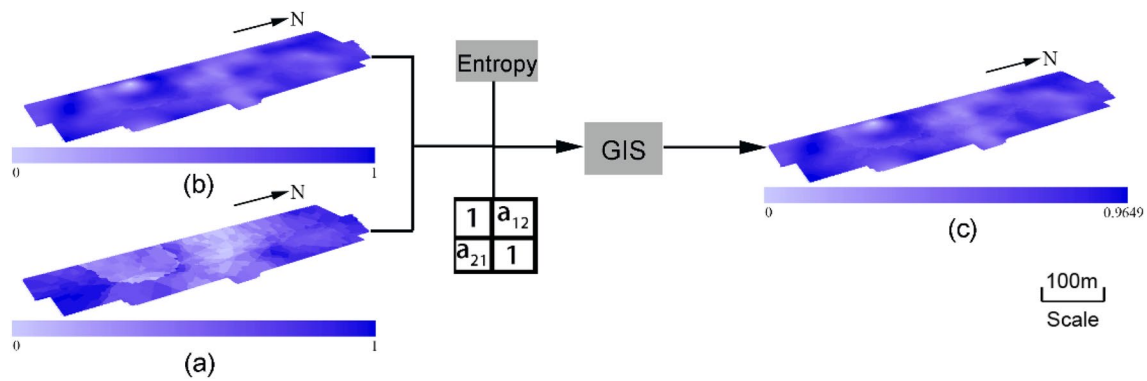


**Fig. 8** Thematic map of criterion layer—mining activity: longwall caving. **a** Mined thickness; **b** height of overburden failure

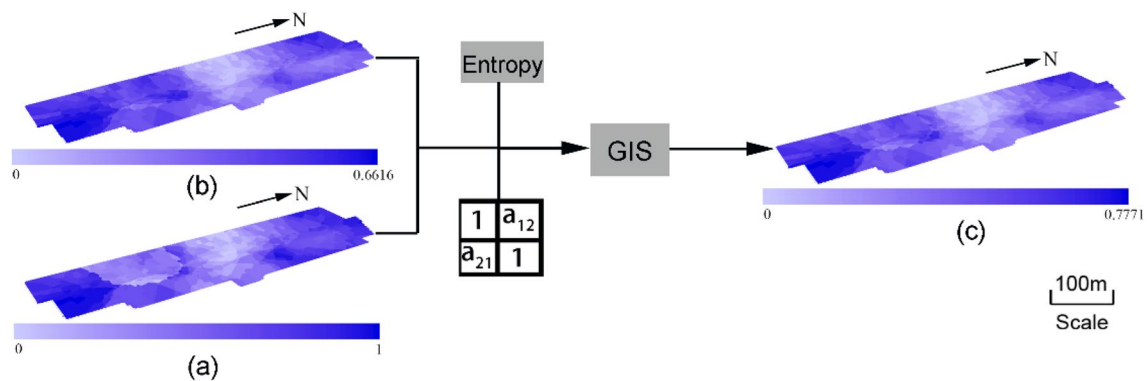


**Fig. 9** Thematic map of criterion layer—mining activity: paste backfill. **a** Mined thickness; **b** height of overburden failure

used on the remaining slices to prevent the development of a water-conducting fractured zone. Moreover, a certain top coal layer was established to effectively increase the thickness of the overburden, which was close to the coal seam outcrop with significant unevenness of the bedrock surface and subject to weathering. Finally, the BMHI was significantly reduced and mining was carried out safely, which indicates that the results of hazard zone mapping were consistent with the actual geological conditions and thus provides effective guidance for practical engineering projects to reduce the inrush hazard.

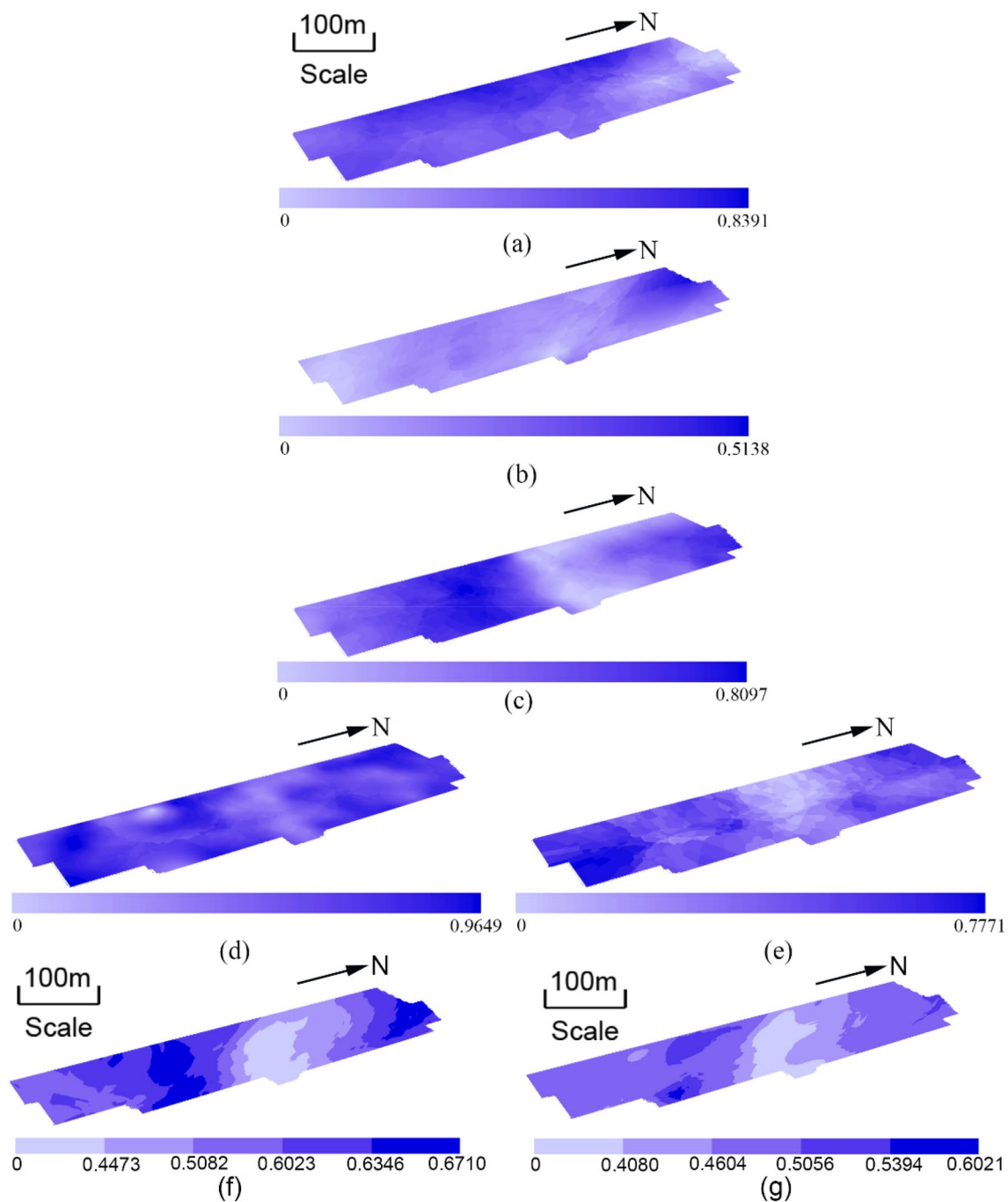
An overlay analysis of the criterion layer was performed using GIS; the calculation process and results are shown in Fig. 10. Then, the criteria layer was quantitatively analyzed to separate the inrush hazard zones in the study area (Fig. 10f, g).

Figure 10g reveals that most of the study area is safe after paste backfilling; the hazard zones were classified using the natural breaks method as  $G = (0.3, 0.45, 0.65, 0.80, \text{ and } 0.95)$ , which are described as follows:

(1) Class A: no inrush hazard. The bedrock is generally more than 29 m thick and the mined thickness is 2.2 m.

The overburden thickness is more than required for ensuring that it is a no-hazard zone.

- (2) Class B: relatively low inrush hazard, which is mainly in the thick bedrock zone. Paste backfilling was carried out under the disturbed overburden and the water-conducting fractured zone did not affect the bottom aquifer in the loose layer.
- (3) Class C: a moderate inrush hazard, mainly in the area with relatively thick bedrock, where the thickness of the clay layer at the bottom of the Quaternary deposits is relatively constant. Furthermore, the aquifer has a low water level.
- (4) Class D: a high inrush hazard, which is mainly in the northeastern region of the study area where the clay layer is thicker but still affected by the density of small faults. Once mining takes place, the inrush hazard may be increased. However, the hazard index is reduced from 0.5082 to 0.6023 with longwall caving to 0.4604–0.5056 with paste backfill based on the results of the mapping of the hazard zone.
- (5) Class E: a very high inrush hazard, which is scattered mainly in the northern part of the study area. The bedrock and clay layer are both thin. In addition, the water



**Fig. 10** Process of overlay analysis and hazard zone map of water and sand intrushes due to mining under aquifer with loose sand. **a** Geological structure; **b** aquifuge; **c** water levels of aquifer; **d** mining activity—longwall caving; **e** mining activity—paste backfill; **f** hazard zone map of longwall caving; and **g** hazard zone map of paste backfill

abundance of the aquifer is moderate. As a result, the thin layer of bedrock can easily fail, thus affecting the loose sand aquifer and even the upper aquifer, which is prone to WSI. The hazard index ranges from 0.6346 to 0.6710 with longwall mining but is reduced to 0.5394–0.6021 with paste backfilling. Therefore, paste backfilling should be used to reduce the intrush hazard.

ity—longwall caving; **e** mining activity—paste backfill; **f** hazard zone map of longwall caving; and **g** hazard zone map of paste backfill

Finally, the BMHI is significantly reduced, which means that mining can be carried out safely, indicating that the results of hazard zone mapping are consistent with the actual geological conditions. This provides effective guidance for practical engineering projects and reduces the intrush hazard with effective technical measures.



## Conclusions

WSIs are mining-induced incidents that occur due to many complex and nonlinear dynamic factors. We quantitatively analyzed the key factors for inrush hazards. A modified AHP was used to construct a quantitative method of analysis with an evaluation index to determine how much paste backfilling reduced the inrush hazard. The evaluation index for the hazard assessment target stratum was divided into four criteria layers: the geological structure, aquifuge, water abundance of the aquifer, and mining activity. Each criterion was then evaluated using eight factors, the: unevenness of the bedrock surface, fractal dimension of faults, thicknesses of the overburden and the clay layer at the bottom of the Quaternary deposits, specific capacity and hydraulic conductivity of the aquifer, mined thickness, and height of overburden failure. Then, a hazard zone map was created based on the criterion layer using an overlay analysis with GIS.

The evaluation indicators were quantified based on a case study of the Taiping coal mine. A modified AHP was combined with the entropy method to determine the weight of each evaluation criterion and factor. The results indicated that paste backfilling effectively reduced the influential weight of the height of overburden failure on the WSI hazard. Then, a thematic map of each criterion that contributes to the hazard was created by calculating the BMHI, based on the weights of the factors. Moreover, a quantitative model of the WSI hazard assessment caused by paste backfilling under an aquifer with loose sand was constructed and used to analyze the hazard zone map. The evaluation results were comparatively analyzed based on longwall caving and paste backfilling. The results showed that the hazard index of Class E (a very high hazard zone) was reduced from 0.6346 to 0.6710 to 0.5394–0.6021 by paste backfilling, and that of Class D (a high-hazard zone) was reduced from 0.5082 to 0.6023 to 0.4604–0.5056, which indicates that paste backfilling reduces the influential weight of the height of overburden failure on the WSI hazard. Backfill plays an important role in controlling movement and failure of the roof, mitigates the development of a water-conducting fractured zone, and effectively reduces the WSI hazard due to coal mining under an aquifer with loose sand.

**Acknowledgements** This study was supported by the National Key Research and Development Program of China under grant 2019YFC1805400 and the Fundamental Research Funds for the Central Universities (2020ZDPY0201). The study was also supported by the Science and Technology Project of Henan Province under grant 212102310596.

## References

Babos HB, Black S, Pluskowski A, Brown A, Rohrsen M, Chappaz A (2019) Evidence for the onset of mining activities during the

- 13th century in Poland using lead isotopes from lake sediment cores. *Sci Total Environ* 683:589–599. <https://doi.org/10.1016/j.scitotenv.2019.05.177>
- Deng X, Zhang J, Zhou N, Wit B, Wang C (2017) Upward slicing longwall-roadway cemented backfilling technology for mining an extra-thick coal seam located under aquifers: a case study. *Environ Earth Sci* 76(23):789. <https://doi.org/10.1007/s12665-017-7120-9>
- Doherty JP, Hasan A, Suazo GH, Fourie A (2015) Investigation of some controllable factors that impact the stress state in cemented paste backfill. *Can Geotech J* 52(12):1901–1912. <https://doi.org/10.1139/cgj-2014-0321>
- Fan K, Li W, Wang Q, Liu S, Xue S, Xie C, Wang Z (2019) Formation mechanism and prediction method of water inrush from separated layers within coal seam mining: a case study in the Shilawusu mining area, China. *Eng Fail Anal* 103:158–172. <https://doi.org/10.1016/j.engfailanal.2019.04.057>
- Hou C, Zhu W, Yan B, Guan K, Niu L (2019) Analytical and experimental study of cemented backfill and pillar interactions. *Int J Geomech* 19(8):1–16. [https://doi.org/10.1061/\(ASCE\)GM.1943-5622.0001441](https://doi.org/10.1061/(ASCE)GM.1943-5622.0001441)
- Huang P, Spearing AJS, Feng J, Jessu KV, Guo S (2018) Effects of solid back filling on overburden strata movement in shallow depth longwall coal mines in west China. *J Geophys Eng* 15:2194–2208. <https://doi.org/10.1088/1742-2140/aac62c>
- Li P, Qian H, Wu J, Chen J (2013) Sensitivity analysis of TOPSIS method in water quality assessment: I. Sensitivity to the parameter weights. *Environ Monit Assess* 185:2453–2461. <https://doi.org/10.1007/s10661-012-2723-9>
- Li H, Bai H, Wu J, Meng Q, Ma K, Wu L, Meng F, Wang S (2019a) A set of methods to predict water inrush from an ordovician karst aquifer: a case study from the Chengzhuang Mine, China. *Mine Water Environ* 38:39–48. <https://doi.org/10.1007/s10230-018-00572-3>
- Li M, Zhang J, Sun K, Wu Z, Zhou N (2019b) Reducing surface subsidence risk using solid waste backfill technique: a case study under buildings. *Pol J Environ Stud* 28(5):3333–3341. <https://doi.org/10.15244/pjoes/94814>
- Li M, Zhang J, Wu Z, Liu Y (2019c) An experimental study of the influence of lithology on compaction behavior of broken waste rock in coal mine backfill. *R Soc Open Sci* 6(4):182205. <https://doi.org/10.1098/rsos.182205>
- Liu J, Sui W, Zhao Q (2017) Environmentally sustainable mining: a case study of intermittent cut-and-fill mining under sand aquifers. *Environ Earth Sci* 76(16):562. <https://doi.org/10.1007/s12665-017-6892-2>
- Polak K, Rózkowski K, Czaja P (2016) Causes and effects of uncontrolled water inrush into a decommissioned mine shaft. *Mine Water Environ* 35(2):128–135. <https://doi.org/10.1007/s10230-015-0360-6>
- Saaty TL (1980) The analytic hierarchy process: planning, priority setting, resource allocation. McGraw-Hill, New York
- State Administration of Coal Mine Safety (2018) Detailed rules for coal mine water prevention. Coal Industry Press, Beijing (**In Chinese**)
- State Administration of Security Supervision, State Administration of Coal Mine Safety, National Energy Administration et al (2017) Code for the retention and compression of coal pillars in buildings, water bodies, railways and main shafts. Coal Industry Press, Beijing (**In Chinese**)
- Sui W, Zhang D, Cui Z, Wu Z, Zhao Q (2015) Environmental implications of mitigating overburden failure and subsidences using paste-like backfill mining: a case study. *Int J Min Reclam Environ* 29(6):521–543. <https://doi.org/10.1080/17480930.2014.969049>
- Sun Q, Zhang J, Zhou N, Qi W (2018) Roadway backfill coal mining to preserve surface water in western China. *Mine Water Environ* 37:366–375. <https://doi.org/10.1007/s10230-017-0466-0>

- Wu Q, Xu H, Pang W (2008) GIS and ANN coupling model: an innovative approach to evaluate vulnerability of karst water inrush in coal mines of north China. *Environ Geol* 54:937–943. <https://doi.org/10.1007/s00254-007-0887-3>
- Wu Q, Liu Y, Liu D, Zhou W (2011) Prediction of floor water inrush: the application of GIS-based AHP vulnerable index method to Donghuantuo coal mine, China. *Rock Mech Rock Eng* 44:591–600. <https://doi.org/10.1007/s00603-011-0146-5>
- Wu J, Li P, Qian H, Chen J (2015) On the sensitivity of entropy weight to sample statistics in assessing water quality: statistical analysis based on large stochastic samples. *Environ Earth Sci* 74(3):2185–2195. <https://doi.org/10.1007/s12665-015-4208-y>
- Xu C, Chen Q, Luo W, Liang L (2019) Analytical solution for estimating the stress state in backfill considering patterns of stress distribution. *Int J Geomech* 19:1–23. [https://doi.org/10.1061/\(ASCE\)GM.1943-5622.0001332](https://doi.org/10.1061/(ASCE)GM.1943-5622.0001332)
- Yang B, Sui W, Duan L (2017) Risk assessment of water inrush in an underground coal mine based on GIS and fuzzy set theory. *Mine Water Environ* 36:617–627. <https://doi.org/10.1007/s10230-017-0457-1>
- Yang B, Sui W, Liu J (2019) Application of GIS-based decision making model to evaluate safety of underground mining under Neogene aquifers. *Int J Oil Gas Coal T* 22(1):40–63. <https://doi.org/10.1504/IJOGCT.2019.102277>
- Zhang J, Jiang H, Deng X, Ju F (2014) Prediction of the height of the water-conducting zone above the mined panel in solid backfill mining. *Mine Water Environ* 33(4):317–326. <https://doi.org/10.1007/s10230-014-0310-8>
- Zhang J, Zhang Q, Sun Q, Gao R, Germain D, Abro S (2015) Surface subsidence control theory and application to backfill coal mining technology. *Environ Earth Sci* 74(2):1439–1448. <https://doi.org/10.1007/s12665-015-4133-0>
- Zhang Y, Cao S, Guo S, Wan T, Wang J (2018) Mechanisms of the development of water-conducting fracture zone in overlying strata during shortwall block backfill mining: a case study in northwestern China. *Environ Earth Sci* 77(14):543. <https://doi.org/10.1007/s12665-018-7726-6>
- Zhu X, Guo G, Zha J, Chen T, Fang Q (2016) Surface dynamic subsidence prediction model of solid backfill mining. *Environ Earth Sci* 75:1–9. <https://doi.org/10.1007/s12665-016-5817-9>
- Zhu X, Guo G, Liu H, Chen T, Yang X (2019) Experimental research on strata movement characteristics of backfill–strip mining using similar material modeling. *Bull Eng Geol Environ* 78(4):2151–2167. <https://doi.org/10.1007/s10064-018-1301-y>

**Publisher's Note** Springer Nature remains neutral with regard to jurisdictional claims in published maps and institutional affiliations.